

# A Performance Model for Bifacial PV Modules

Daniel Riley<sup>1</sup>, Clifford Hansen<sup>1</sup>, Joshua Stein<sup>1</sup>, Matthew Lave<sup>1</sup>, Johnson Kallickal<sup>1</sup>, Bill Marion<sup>2</sup>,  
Fatima Toor<sup>3</sup>

<sup>1</sup>Sandia National Laboratories, Albuquerque, NM, USA

<sup>2</sup>National Renewable Energy Laboratory, Golden, CO, USA

<sup>3</sup>The University of Iowa, Iowa City, IA, USA

**Abstract** — Sandia National Laboratories, the National Renewable Energy Laboratory, and the University of Iowa are collaborating to develop a performance model for bifacial PV modules. As with monofacial PV modules, a bifacial PV model consists of sequential operation of the component sub-models. Bifacial PV modules accept light on both their front and rear surfaces which presents a unique modeling challenge. This paper describes the approach of Sandia, NREL, and the University of Iowa to create a bifacial PV model and verify its accuracy with measured field data.

**Index Terms** — photovoltaic modules, bifacial, model, performance

## I. INTRODUCTION

Bifacial photovoltaic (PV) modules can accept light on both the front and rear surfaces. Currently, efforts are being put forth to describe, test, rate, and model bifacial PV modules. As bifacial PV becomes a larger portion of the overall PV market. Sandia National Laboratories (Sandia), the National Renewable Energy Laboratory (NREL) and the University of Iowa are working together to provide the necessary data and analysis to better describe and predict bifacial PV performance to facilitate wider adoption throughout the PV market.

Sandia is a leader in the photovoltaic (PV) modeling community in both the development and evaluation of PV performance models. Sandia is leading this effort to develop performance models for bifacial PV modules and systems, with the ultimate goal of creating a highly accurate and computationally convenient model to predict the output of a bifacial PV system under any weather conditions. In addition to the weather data, system information must also be provided to the model.

This paper describes the progress of Sandia's efforts towards an accurate bifacial PV performance model.

## II. MODELING APPROACH

The overall approach for modeling bifacial PV systems comprises a sequence of sub-models similar to the approach employed for modeling monofacial PV. Initial models for irradiance translation and/or decomposition are followed by models describing the effects of shading, irradiance spectrum, and soiling. PV cell temperature is estimated using a cell temperature model; cell temperature and incident irradiance

are then used within the PV module performance model. Effects of mismatched output among cells and modules may be calculated in order to estimate the DC output of an entire PV string.

### A. Front and Rear Irradiance

The irradiance available for the front surface of bifacial PV modules is modeled in the same manner as for monofacial PV. Direct and diffuse irradiance are transposed onto a tilted surface, and the site albedo can be used to estimate the amount of ground-reflected light present on the front surface.

Determining the irradiance on the rear side of a PV module, however, is a relatively new area. The rear side irradiance will be affected by the albedo of the ground and nearby surfaces and by the irradiance on these surfaces. However, additional factors such as the module's position within a row, the row's height above ground, the proximity of the row to other rows or structures, the transparency of the module [1], and the shadow pattern on the ground alter the amount of irradiance available to the rear side of a bifacial PV module. Several efforts are underway to develop and validate rear-side irradiance models [2]. Sandia is developing a view factor model for irradiance on each cell that accounts for 3D geometry [3]; NREL [4] and SunPower [5] are proposing array-scale models with 2D geometry for fixed and single axis tracking systems, respectively; and Univ. of Iowa is pursuing models using ray-tracing that account for row-to-row effects [6]. Selecting the best method for determining rear irradiance may depend on the use case and requirements for computation time, accuracy, and resolution.

### B. Soiling, Shading, Spectrum

We expect that the effects of soiling on bifacial PV will be similar to those observed for monofacial PV, or perhaps reduced somewhat when bifacial PV modules are mounted so that little soil accumulates on the rear side of the module.

PV racking, junction boxes, or module wiring may shade parts of the rear-side of a bifacial PV module from irradiance sources. As we expect most of the irradiance on the rear-side of a bifacial PV module (in a typical mounting orientation to monofacial modules) to comprise diffuse reflected and sky diffuse irradiance, we anticipate that shading on the rear side will reduce rear-side irradiance in proportion to the shaded area relative to the module area.

### III. VERIFICATION AND ANALYSIS

The spectrum of the incident light on the front side affects the module's output, and the effect of spectrum changes can be estimated with existing models, e.g., [7, 8]. Spectral irradiance on the rear side can differ from irradiance on the front side due to absorption at the surfaces reflecting the light reaching the rear-side. We suspect that the effect on module output from the variation in irradiance spectrum on the rear surface is small compared to the effect of irradiance spectrum on the front surface irradiance. In the future, spectral reflection data for various surfaces can be analyzed to quantify the impact of variation in rear side spectral irradiance.

#### C. Cell Temperature

For monofacial PV system models, cell temperature is generally modeled from the incident irradiance, the ambient air temperature, the wind speed and possibly other factors such as wind direction, cell location, or module efficiency, e.g., [7]. We expect that bifacial PV modules will have similar thermal characteristics as monofacial PV, although a rear-irradiance term may need to be included in the factors which affect temperature.

#### D. Electrical Performance

The electrical output of a PV module for given irradiance, cell temperature, and other factors is described by the module's I-V curve. An electrical performance model can model the I-V curve or, at least, important points on the I-V curve such as  $I_{SC}$ ,  $V_{OC}$ ,  $I_{MP}$ , and  $V_{MP}$ . We hope that electrical performance models for bifacial PV modules will resemble those used for monofacial modules, e.g., a diode-model capable of recreating a whole I-V curve [9], or a point-value model such as the Sandia Array Performance Model (SAPM) [7] that estimates a few important points on the I-V curve. However, as we show in this paper, bifacial modules may inherently exhibit characteristics of shaded monofacial modules due to shading from nearby structure such as racking, which complicates PV power modeling.

#### E. Cell and Module Mismatch

Mismatched output of cells within a module, and of modules in a string, is caused primarily by differing irradiance conditions along the string, and secondarily by intrinsic differences among the cells. When the cells in a string produce differing levels of current the performance of the string suffers due to mismatch. In monofacial PV systems, the level of current mismatch between modules must be quite high in order to have a significant effect on the power of the string. While the same underlying principles hold for bifacial modules, the possible variation in irradiance among cells is affected by variation of rear-side irradiance across the cells, which can be substantial [2].

Sandia is generating data sets and analysis tools to verify some of the sub-models comprising the bifacial PV performance model, demonstrate the applicability of existing monofacial PV models where bifacial PV performance is not significantly different, and develop new bifacial performance models where existing monofacial models fail to predict bifacial PV performance.

Sandia and NREL have each constructed test arrays and equipment to provide data that will be used to verify the models, such as Sandia's 4-tilt bifacial test shown in Fig. 1. The test bed contains both bifacial and monofacial PV modules at a range of tilt angles for a direct comparison of the performance of monofacial and bifacial technologies.



Fig. 1. Sandia's 4-tilt test bed. Rows are tilted between 15 and 45 degrees with rear irradiance sensors at the top and bottom of each row, near the center of the row.

#### A. Front and Rear Irradiance

The rear irradiance models developed by NREL, University of Iowa, and Sandia National Laboratories are presented in other papers [3, 4, 6].

Empirical data to validate these models are being collected on several test arrays including fixed tilt, single axis trackers, and dual axis trackers. For models that allow for prediction of different illumination across the rear of a PV module, Sandia has created the high spatial resolution rear irradiance module (HSRRIM) shown in Fig 2. The module has a form factor similar to a PV module that can be easily moved and placed anywhere within an array or around the SNL site. The HSRRIM has 10 calibrated reference cells which measure the rear side irradiance pattern across the back of the module.

Rear irradiance readings from the HSRRIM show that the distribution of unobstructed rear irradiances across the back of a bifacial PV module can vary greatly depending on the module's height above ground, tilt angle, and the surface below the module. An installation at latitude tilt with the HSRRIM 0.6 meters above the ground can produce variations in rear irradiance above  $50 \text{ W/m}^2$  between cells on a sunny day.



Fig. 2. Sandia's high spatial resolution rear irradiance module. A sensor with PV module form factor and ten reference cells measuring rear irradiance

### B. Rear Side Shading

To empirically determine the effect of rear-side shading, we performed a series of tests where a percentage of the rear side of a bifacial module was obscured, an I-V curve was measured, then the obstruction was removed and a second I-V curve was measured. The two I-V curves are separated by less than 1 minute such that the front and rear irradiance varied by less than 0.25% between curves. The obstruction's size, orientation, location, and distance from module were varied and the effect on the I-V curve was noted. For the following plots, the obstruction's orientation was either in "direction A" which crossed all of module's cell strings, or in "direction B" which placed the obstruction behind only one cell string. When the obstruction is directly against the back of the module this is denoted as "hard shade", and when the obstruction was approximately 5.9 cm from the back of the module is denoted as "soft shade". Fig. 3 shows an example of a 20% hard shade obstruction in direction B, and Fig. 4 shows an I-V curve with the obstruction and an I-V curve after the obstruction was removed.



Fig. 3. The obstruction behind a bifacial PV module in "direction B" with 20% coverage. Obstruction is in contact with the rear surface of the PV.

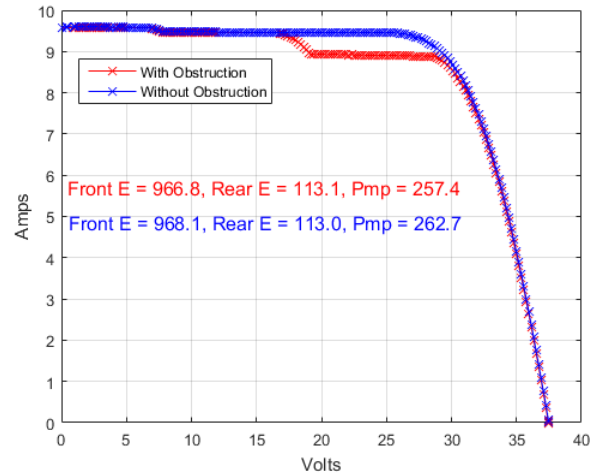


Fig. 4. An I-V curve of a bifacial module with (red) and without (blue) an obstruction.  $P_{MP}$  difference  $\approx 2\%$ .

The object of the testing is to formulate a model to predict the impact on PV performance of various factors relating to obstructions on the rear side of the PV module, such as racking. We found that obstructions can greatly affect the  $I_{SC}$  of the PV in a complicated manner. Fig. 5 shows the change in  $I_{SC}$  related to an obstruction's orientation, size, and distance from the PV. It is clear that the  $I_{SC}$  is greatly influenced by the orientation of the obstruction, i.e. whether it covers one cell string or all cell strings. However, Fig. 6 shows that  $P_{MP}$  is generally reduced in proportion to the obstructed area, and that the orientation of the obstruction does not greatly affect the  $P_{MP}$ .

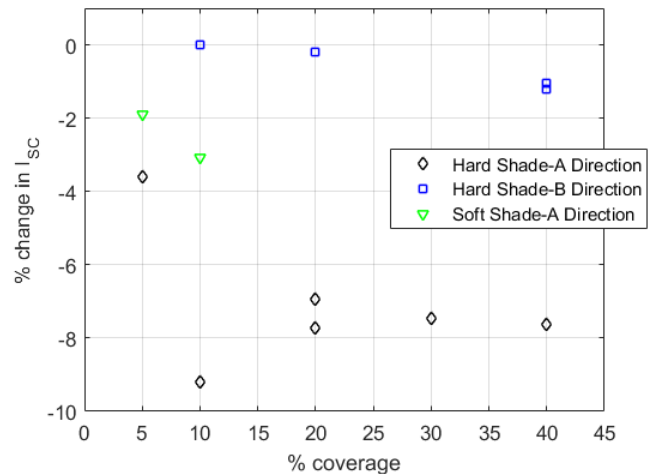


Fig. 5.  $I_{SC}$  changes from without obstruction to obstruction. Great changes in  $I_{SC}$  depending on the direction of the obstruction.

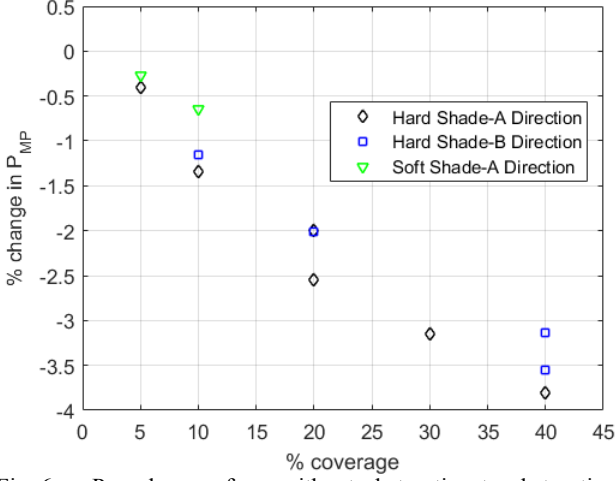


Fig. 6.  $P_{MP}$  changes from without obstruction to obstruction as a function of the size of the obstruction relative to the module size.

It is clear that when obstructions block the rear side of a PV module, it is impractical to use  $I_{SC}$  as an estimator of the amount of power a bifacial PV module may create since losses in  $I_{SC}$  and  $P_{MP}$  are not well correlated. For this reason we propose a model to estimate the effect of obstructions on  $P_{MP}$ , rather than predict effects on  $I_{SC}$  and then use  $I_{SC}$  to predict  $P_{MP}$  (as is typical in some monofacial models, e.g. [7]). A secondary factor seems to be the distance of the obstruction from the rear of the PV module.

If we assume that the irradiance striking the rear side of a bifacial PV module is proportional to the power generated from that irradiance, we develop (1) to estimate the reduction in  $P_{MP}$  due to some amount of obstruction.

$$D_{Obs} = -E_{rear} \times BiFi_{Pmp} \times CoverageRatio \quad (1)$$

where  $D_{Obs}$  is the reduction in  $P_{MP}$  (unitless),  $E_{front}$  and  $E_{rear}$  are the irradiance on the front and rear,  $BiFi_{Pmp}$  is the bifaciality (the ratio of power produced by the rear side to the front side under identical illumination and temperature) measured as in [1], and  $CoverageRatio$  is the ratio of the obstruction size to the module's active area.

Fig. 7 shows the result of using (1) compared to a least squares fit of different measured data points. The model equation estimates slightly more loss than is observed in a "hard shade" scenario. We believe that a simple scaling factor may be applied to (1) to account for an obstruction's distance from the rear of the PV module. Additional testing at various obstruction distances is required in order to determine an appropriate scale factor.

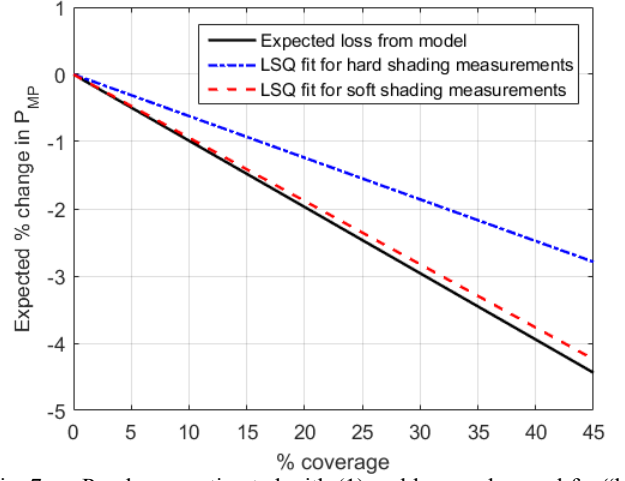


Fig. 7.  $P_{MP}$  losses estimated with (1) and losses observed for "hard shade" and "soft shade".

### C. Cell and Module Temperature

Module temperature models such as in [7] estimate a module temperature from environmental factors and a module's thermal characteristics. We have collected module temperature and environmental data from a number of co-located bifacial and monofacial systems in order to determine the applicability of existing temperature models to bifacial PV.

Equation (2) presents one simple model that has proven adequate at estimating steady state PV module temperatures:

$$T_{Module} = E \cdot \left[ e^{a+b \cdot WS} \right] + T_{ambient} \quad (2)$$

Fig. 8 shows the results of modeling a bifacial PV system temperature with (2). Residual plots of the errors for a co-located monofacial system exhibit nearly identical features and residual magnitudes. It is clear that the model is descriptive of this bifacial PV system which we regard as typical; the RMSE of the model for the bifacial system is about 3.4 °C, while the RMSE for a co-located monofacial system is 3.1 °C.



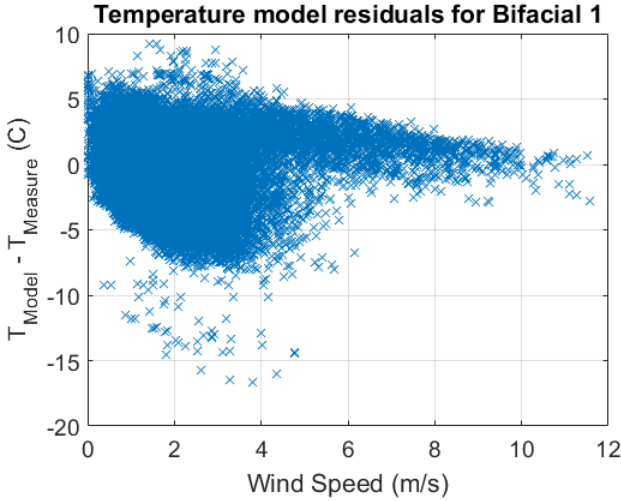


Fig. 8. Module temperature residuals as a function of wind speed for a bifacial system.

The accumulated system and module data has provided us with confidence that a simple model such as (2) will be sufficient for modeling bifacial module temperature as a function of irradiance, wind speed, and ambient temperature; even when using the typical parameters determined from monofacial modules.

#### D. Electrical performance

We propose a simple model for bifacial PV power, leaving a more complicated model for other points of interest, e.g.,  $V_{MP}$ , to future work. We estimate maximum power for a bifacial module from the front irradiance, rear irradiance, cell temperature, module bifaciality, module temperature coefficient, and the nominal power of the PV module under STC conditions.

$$\begin{aligned}
 P_{MP} = P_{MP0} \times & \left[ 1 + \gamma_{Pmp} \times (T_{Cell} - T_0) \right] \\
 & \times \frac{E_f + Bifi_{Pmp} \times E_r}{E_0} \\
 & \times (1 + D_{obs})
 \end{aligned} \quad (3)$$

where:

$P_{MP0}$  is the maximum power at reference conditions

$\gamma_{Pmp}$  is the maximum power temperature coefficient

$T_{Cell}$  is the cell temperature

$T_0$  is the reference cell temperature

$E_f$  is the average front side irradiance

$E_r$  is the average rear side irradiance

$E_0$  is the reference irradiance

$Bifi_{Pmp}$  is the bifaciality of the PV module's  $P_{MP}$  as in [1]

$D_{obs}$  is a derate (unitless) based on the amount of rear side obstruction as shown in (1)

Eq. 3 ignores smaller effects such as from spectrum variation and mismatch. These smaller effects may be incorporated in the future.

Fig. 9 compares the modeled and measured maximum power for one single bifacial PV module shown in Fig. 10. The front irradiance is measured by a coplanar reference cell, and the rear irradiance is estimated by averaging two reference cells adjacent to the module's western edge. The simple model predicts the module power to within 5 watts of the measured power of a single bifacial PV module with no rear obstructions when the module is producing less than 200 watts. However, the errors increase to about 20 watts at higher power levels.

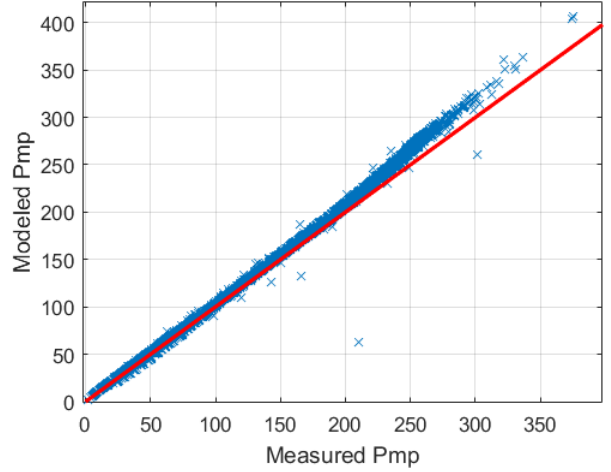


Fig. 9. Modeled and measured maximum power from (3) for a single bifacial PV module over 25 days, 1:1 line shown in red



Fig. 10. Bifacial PV module under test circled in red. Rear irradiance reference cells shown with green triangles

Analysis of the model residuals shows that the model is strongly over-predicting at midday when module temperatures are high as shown in Fig. 11. The residuals may indicate an error in the temperature coefficient for power; however, the nonlinear behavior of the residuals indicates that there may be several physical causes for the model errors.

## V. ACKNOWLEDGEMENTS

Sandia National Laboratories is a multi-mission laboratory managed and operated by National Technology & Engineering Solutions of Sandia, LLC., a wholly owned subsidiary of Honeywell International, Inc., for the U.S. Department of Energy's National Nuclear Security Administration under contract DE-NA0003525.

## REFERENCES

- [1] C. Deline, S. MacAlpine, B. Marion, F. Toor, A. Asgharzadeh, and J. S. Stein, "Evaluation and field assessment of bifacial photovoltaic module power rating methodologies," in *2016 IEEE 43rd Photovoltaic Specialists Conference (PVSC)*, 2016, pp. 3698-3703.
- [2] C. W. Hansen, J. S. Stein, C. Deline, S. MacAlpine, B. Marion, A. Asgharzadeh, *et al.*, "Analysis of irradiance models for bifacial PV modules," in *2016 IEEE 43rd Photovoltaic Specialists Conference (PVSC)*, 2016, pp. 0138-0143.
- [3] C. W. Hansen, D. M. Riley, "A Computationally Efficient Method for Detailed Modeling of Rear-Side Irradiance for Bifacial PV Modules," in *2017 IEEE 44th Photovoltaic Specialists Conference (PVSC)*, 2017.
- [4] B. Marion, S. MacAlpine, C. Deline, A. Asgharzadeh, F. Toor, D. Riley, J. Stein, C. Hansen, "An Irradiance Model for Bifacial PV Modules," submitted to *2017 IEEE 44th Photovoltaic Specialists Conference (PVSC)*, 2017.
- [5] M. A. Anoma, J. Scholl, B. Bourne, D. Jacob, "2D View Factor Model and Validation for Bifacial PV and Diffuse Shade on Single-Axis Trackers," in *2017 IEEE 44th Photovoltaic Specialists Conference (PVSC)*, 2017.
- [6] A. Asgharzadeh, T. Lubenow, J. Sink, B. Marion, *et al.*, "Analysis of the Impact of Installation Parameters and System Size on Bifacial Gain and Energy Yield of PV Systems," in *2017 IEEE 44th Photovoltaic Specialists Conference (PVSC)*, 2017.
- [7] D. King, W. Boyson, and J. Kratochvil, "Photovoltaic Array Performance Model". SAND2004-3535, 2004.
- [8] M. Lee, A. Panchula, "Spectral Correction for Photovoltaic Module Performance Based on Air Mass and Precipitable Water," in *2016 IEEE 43rd Photovoltaic Specialists Conference (PVSC)*, 2016.
- [9] W. De Soto, S. A. Klein, W. A. Beckman, "Improvement and Validation of a Model for Photovoltaic Array Performance," *Solar Energy*, vol. 80, pp. 78-88, 2006.

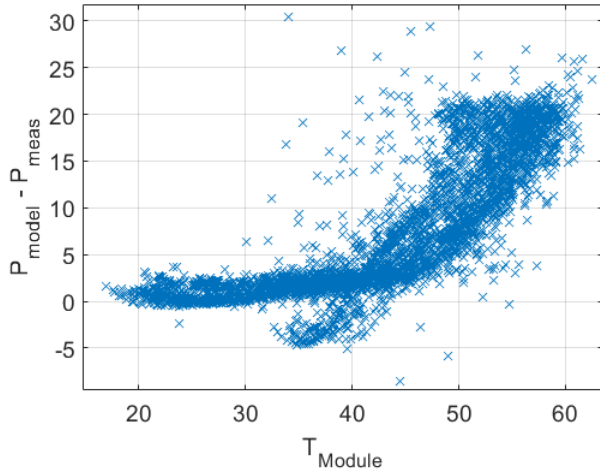


Fig. 11. Bifacial PV model residuals show an over-prediction at high temperatures

## IV. CONCLUSION AND FUTURE WORK

Existing models for determination of cell and module temperature of monofacial PV modules have been confirmed to also provide good results for bifacial PV modules and we recommend their further use in bifacial PV modeling.

A new derate factor may be needed for bifacial PV systems to account for reduced rear side irradiance due to racking or other obstructions. A simple factor based on the coverage ratio of the rear side of the module could be sufficient for modeling power loss due to obstructions.

Finally, the simple power model for bifacial modules presented in (3) provides errors of approximately 2% at low power levels, with increasing errors up to about 8% at high power levels. It is clear that (3) is not adequately capturing all of the physical effects that influence bifacial PV module performance, and additional factors must be identified or improved in order to develop a more accurate model.